



# A Data-driven Modeling Approach for Water Flow Dynamics in Soil

Zeyuan Song<sup>a</sup>, Zheyu Jiang<sup>a\*</sup>

<sup>a</sup>*Oklahoma State University, 420 Engineering North, Stillwater, Oklahoma 74074 USA*  
Corresponding author: [zheyu.jiang@okstate.edu](mailto:zheyu.jiang@okstate.edu)

## Abstract

Modeling and predicting soil moisture is essential for precision agriculture, smart irrigation, drought prevention, etc. Estimating root zone soil moisture from surface or near-surface soil moisture data is typically achieved by solving a hydrological model that describes water movement through soils. Advanced agro-hydrological models today use the Richards equation, a highly nonlinear, degenerate elliptic-parabolic partial differential equation that captures irrigation, precipitation, evapotranspiration, runoff, and drainage. State-of-the-art Richards equation solvers employ either a finite difference, finite element, or finite volume discretization framework in space. In this paper, we introduce a novel computational framework to solve generic  $n$ -dimensional Richards equation by introducing global random walk and deep neural network to a modified finite volume method (FVM). Furthermore, for  $n$ -dimensional Richards equation, we introduce multi-point flux approximation to the FVM framework. Through these innovations, our novel computational framework effectively utilizes the underlying physics behind the Richards equation, which enhances the speed and accuracy of the solution process. Through an illustrative case study, we demonstrate the efficiency and effectiveness of our computational framework and show that it correctly characterizes the physical relationships among soil moisture content, pressure head, and flux.

**Keywords:** Soil moisture, Richards equation, finite volume method, neural network, random walk

## 1. Introduction

Soil moisture is a key hydrological parameter that has significant importance to human society and environment. Accurate modeling and monitoring of soil moisture in crop fields, especially in the root zone (top 100 cm of soil), is essential for improving agricultural production and crop yield with the help of precision irrigation and farming tools. Recent studies also show that monitoring root zone soil moisture at suitable locations and adjusting irrigation schedules accordingly can reduce water use by 40-60% (Sadler et al., 2005). Improved irrigation infrastructures based on soil moisture knowledge could also prevent more than \$30 billion/year in drought related agricultural losses in the US (Khand et al., 2018). This is especially important to US states like Oklahoma, where 41% of total water use goes directly to agricultural irrigation and almost 90% of the land area suffers from drought throughout the year (Droughts.gov, 2022). Estimating root zone soil moisture is typically achieved by solving a hydrological model that describes water movement through soils. Most of the advanced agro-hydrological models today incorporate the Richards equation (Richards, 1931), which captures irrigation, precipitation, evapotranspiration, runoff, and drainage dynamics of water in saturated and unsaturated porous medium such as soil:

$$\frac{\partial \theta(\varphi)}{\partial t} = \nabla \cdot [K(\theta) \nabla(\varphi + z)] - S \quad (1)$$

where  $\varphi$  stands for pressure head,  $\theta$  denotes the soil moisture content,  $K$  is unsaturated hydraulic water conductivity,  $t \in [0, T]$  denotes the time,  $z$  denotes the vertical depth, and  $S$  is the sink term associated with root water extraction, which we ignore without loss of generality. The flux is given by the Darcy's law:  $q = -K(\theta) \nabla(\varphi + z)$ . For unsaturated flow, both  $K$  and  $\theta$  are highly nonlinear functions of  $\varphi$ . For instance, the widely used van Genuchten-Mualem correlations (van Genuchten, 1980) for  $\theta(\varphi)$  and  $K(\theta)$  are:

$$\theta(\varphi) = \begin{cases} \frac{\theta_s - \theta_r}{[1 + (\alpha|\varphi|)^n]^{\frac{n-1}{n}}} + \theta_r, & \varphi < 0 \\ \theta_s, & \varphi \geq 0 \end{cases} \quad (2)$$

$$K(\theta) = K_s \sqrt{\frac{\theta - \theta_r}{\theta_s - \theta_r}} \left\{ 1 - \left[ 1 - \left( \frac{\theta - \theta_r}{\theta_s - \theta_r} \right)^{\frac{n}{n-1}} \right]^{\frac{n-1}{n}} \right\}^2$$

where  $\alpha$  and  $n$  are van Genuchten parameters characterizing different soils, and  $\theta_s$ ,  $K_s$  and  $\theta_r$  denote saturation soil moisture, residual water content, and saturated hydraulic conductivity, respectively. As a result, exact analytical solutions to Equation (1) often do not exist, and numerical solutions rely on discretization of spatial and temporal domains. In particular, the finite volume method (FVM) adopts an integral form of the Richards equation, which captures some valuable physical insights about water flow dynamics (Rathfelder and Abriola, 1994). In addition, FVM is a flexible framework that can be coupled with various other techniques such as the predictor-corrector method (Lai and Ogden, 2015), linearization scheme (Radu et al., 2015), and **global random walk approach** (Vamos, 2013). Recently, we developed a computationally efficient FVM-based framework for solving the Richards equation by integrating it with adaptive linearization scheme, global random walk method, and multi-layer neural networks (Song and Jiang, 2023). In an illustrative example, we showed that our novel data-driven framework not only generated fast and accurate solutions to the 1-D Richards equation, but also implicitly captured the underlying physical relationships among soil moisture content, pressure head, and flux. In this work, we generalize this computational framework to successfully **solving 3-D Richards equation for the first time in the literature.**

## 2. FVM Discretization

To apply FVM to Richards equation, we first integrate both sides of Equation (1) to obtain an integral form of the Richards equation over a higher-dimensional control  $V$ :

$$\int_V \frac{\partial \theta(\varphi)}{\partial t} dV = \int_V \nabla \cdot [K(\theta) \nabla(\varphi + z)] dV \quad (3)$$

Next, we can apply the divergence theorem to convert the volume integral on the RHS of Equation (3) into a surface integral over  $S_V$  by introducing the outward pointing unit normal vector denoted as  $\mathbf{n}$ :

$$\int_V \frac{\partial \theta(\varphi)}{\partial t} dV = \int_{S_V} [K(\theta) \nabla(\varphi + z)] \cdot \mathbf{n} dS_V \quad (4)$$

By doing so, FVM is able to incorporate conservation laws, whereas other discretization methods cannot. Specifically, to obtain the discretized version of Equation (4) using FVM,

we discretize the volume integral on the LHS of Equation (4) into a total of  $N_V$  small cells  $V_i$  with  $i = 1, \dots, N_\omega$  whose volume is denoted as  $\vartheta_i$ . Each  $V_i$  is associated with surfaces  $\omega_{i,j}$  for  $j = 1, \dots, N_{\omega_i}$  on the RHS of Equation (4) whose area is denoted as  $\mathcal{A}(\omega_{i,j})$ , and we use  $[\cdot]_{\omega_i}$  and  $\mathbf{n}_{\omega_i}$  respectively to denote the operator and outward pointing unit normal vector associated with  $\omega_{i,j}$  upon discretization. Next, to discretize the time domain, we approximate the time derivative  $\partial\theta(\varphi)$  as  $\frac{\theta_i^{m+1,s+1} - \theta_i^m}{\Delta t}$ , where  $\theta_i^{m+1,s+1}$  represents the discretized  $\theta$  in the  $i$ th small cell at the next time step  $m + 1$  and iteration step  $s + 1$ , whereas  $\theta_i^m$  is the converged  $\theta$  value in the  $i$ th small cell at the current time step  $m$ . With this, the discretized version of Equation (4) using FVM becomes:

$$\frac{\theta_i^{m+1,s+1} - \theta_i^m}{\Delta t} \vartheta_i = \sum_{j=1}^{N_{\omega_i}} [K(\theta) \nabla(\varphi + z)]_{\omega_{i,j}} \cdot \mathbf{n}_{\omega_{i,j}} \mathcal{A}(\omega_{i,j}) \quad (5)$$

### 3. Data-Driven Global Random Walk Algorithm

In this section, we introduce a data-driven global random walk (DGRW) approach that seeks to implicitly encapsulate the physical knowledge describing particle movement and conservation within a control volume. Global random walk allows particles to move to neighboring cells simultaneously on any direction or stay in their current cells with a given probability. Thus, in 3-D case, there are a total of seven options for every particle. Let  $n_{i,j,k}^{m,s}$  be the number of particles in the cell  $(i, j, k)$  at fixed-point iteration step  $s$  and time step  $m$ . Correspondingly,  $\delta n_{i',j',k'}^{m,s}$ , where  $i' = i - 1, i, i + 1$ ,  $j' = j - 1, j, j + 1$ , and  $k' = k - 1, k, k + 1$ , denotes the number of particles moving from cell  $(i', j', k')$  to cell  $(i, j, k)$ . Explicitly, we can write:

$$n_{i,j,k}^{m,s+1} = \delta n_{i+1,j,k}^{m,s} + \delta n_{i-1,j,k}^{m,s} + \delta n_{i,j+1,k}^{m,s} + \delta n_{i,j-1,k}^{m,s} + \delta n_{i,j,k+1}^{m,s} + \delta n_{i,j,k-1}^{m,s} + n_{i,j,k}^{m,s} \quad (6)$$

As we may expect, having such physical knowledge is important for solving Richards equation, which governs the movement of water molecules in unsaturated and saturated soil systems. In fact, Suci et al. (2021) adopted global random walk concepts and proposed a numerical framework for solving 1- and 2-D Richards equation. In their numerical framework, the authors assumed that the pressure head  $\varphi$  is proportional to the number of particles  $n$  in a cell or control volume. With this assumption, soil moisture content in the cell of interest is simply proportional to the arithmetic mean of the number of particles. While this assumption is valid for diffusion equations (Vamoş et al., 2001), Richards equation is a highly nonlinear convection-diffusion equation, and the exact relationship between  $\varphi$  and  $n$  remains unclear. In fact, we have shown that the numerical framework proposed by Suci et al. (2021) failed to obtain an accurate solution for 1-D Richards equation (Song and Jiang, 2023).

Since the relationship between  $\varphi$  and  $n$  may not be describable by any basic function, we decide to model the relationship using two multi-layer neural networks (MNNs). Although deep neural network with more layers and neurons could also be used, it is not required as MNN with less number of layers (e.g., 3) is sufficient for learning the relationship between  $\varphi$  and  $n$  given enough neurons in the neural network (Hornik, 1991). In one of the MNNs, we approximate  $\varphi$  as a function of  $n$ ,  $\varphi_{i,j,k} = f(n_{i,j,k})$ , at each fixed time step and iteration step. In the other MNN, we learn the inverse mapping

$f^{-1}$  from pressure head information to the number of particles,  $n_{i,j,k} = f^{-1}(\varphi_{i,j,k})$ . During offline training, we first obtain reference solutions from the global random walk solvers developed by Sucui et al. (2021) (code available at GitHub repository: <https://github.com/PMFlow/FlowBenchmark>). We then add Gaussian noise to these reference solutions to 1) account for the possibly nonlinear relationship between  $\varphi$  and  $n$ , and 2) enhance its generalization performance and the quality of solution obtained (Song and Jiang, 2023). Once offline training is complete, we substitute  $f$  to Equation (5) and derive the following data-driven random walk formulation for the discretized Richards equation:

$$n_{i,j,k}^{m,s+1} = \left[ 1 - \left( r_{i+\frac{1}{2},j,k}^{m,s} + r_{i-\frac{1}{2},j,k}^{m,s} + r_{i,j+\frac{1}{2},k}^{m,s} + r_{i,j-\frac{1}{2},k}^{m,s} + r_{i,j,k+\frac{1}{2}}^{m,s} + r_{i,j,k-\frac{1}{2}}^{m,s} \right) \right] n_{i,j,k}^{m,s} \\ + r_{i+\frac{1}{2},j,k}^{m,s} n_{i+1,j,k}^{m,s} + r_{i-\frac{1}{2},j,k}^{m,s} n_{i-1,j,k}^{m,s} + r_{i,j+\frac{1}{2},k}^{m,s} n_{i,j+1,k}^{m,s} + r_{i,j-\frac{1}{2},k}^{m,s} n_{i,j-1,k}^{m,s} \\ + r_{i,j,k+\frac{1}{2}}^{m,s} n_{i,j,k+1}^{m,s} + r_{i,j,k-\frac{1}{2}}^{m,s} n_{i,j,k-1}^{m,s} \quad (6) \\ + f^{-1} \left( \left( r_{i,j,k+\frac{1}{2}}^{m,s} - r_{i,j,k-\frac{1}{2}}^{m,s} \right) \Delta z - \frac{\theta^{m,s}(n_{i,j,k}^{m,s}) - \theta^{m-1}(n_{i,j,k}^{m-1,s})}{L_{i,j,k}^{m,s}} \right)$$

$$\text{where } r_{i\pm\frac{1}{2},j,k}^{m,s} = \frac{K \left( \theta \left( \varphi_{i\pm\frac{1}{2},j,k}^{m,s} \right) \right) \Delta t}{(\Delta x)^2 L_{i\pm\frac{1}{2},j,k}^{m,s}}, \quad r_{i,j\pm\frac{1}{2},k}^{m,s} = \frac{K \left( \theta \left( \varphi_{i,j\pm\frac{1}{2},k}^{m,s} \right) \right) \Delta t}{(\Delta y)^2 L_{i,j\pm\frac{1}{2},k}^{m,s}}, \quad \text{and } r_{i,j,k\pm\frac{1}{2}}^{m,s} = \frac{K \left( \theta \left( \varphi_{i,j,k\pm\frac{1}{2}}^{m,s} \right) \right) \Delta t}{(\Delta z)^2 L_{i,j,k\pm\frac{1}{2}}^{m,s}}.$$

Here, we adopt an adaptive linearization scheme inspired by Mitra and Pop (2019) by adding the term  $L_{i,j,k}^{m,s}(\varphi_{i,j,k}^{m,s+1} - \varphi_{i,j,k}^{m,s})$  on the LHS of Equation (5).

In DGRW algorithm, Equation (6) passes through the inverse mapping  $f^{-1}$  learned from MNN to generate Richards equation solutions in terms of the particle distribution in each cell,  $n_{i,j,k}$ . To convert these solutions to physically meaningful solutions such as the pressure head, flux, and soil moisture content, we apply the trained mapping  $f^{-1}$  and Equation (2). We have proven that the DGRW algorithm is convergent, and the total error

can be estimated using  $\varepsilon = \max_i \left\{ \frac{\|f(n_{i,j,k}^{m,s+1}) - f(n_{i,j,k}^{m,s})\|_F}{\|f(n_{i,j,k}^{m,s+1})\|_F} \right\} = \max_i \left\{ \frac{\|\psi_{i,j,k}^{m,s+1} - \psi_{i,j,k}^{m,s}\|_F}{\|\psi_{i,j,k}^{m,s+1}\|_F} \right\}$ , where  $\|\cdot\|_F$  is the Frobenius norm.

#### 4. An Illustrative Case Study

We modify the 2-D benchmark problem of Haverkamp (1977) that describes groundwater reservoir recharge from a drainage trench by extending it to 3-D. The boundary conditions of the problem are set up as  $\Omega = [0\text{m}, 2\text{m}]^3$ , and  $\Gamma_D = \Gamma_{D_1} \cup \Gamma_{D_2} \cup \Gamma_{D_3} \cup \Gamma_{D_4}$ , in which:

$$\Gamma_{D_1} = \{(x, y, z) \in \partial\Omega | x \in [0\text{m}, 1\text{m}] \wedge y \in \Omega \wedge z = 2\text{m}\},$$

$$\Gamma_{D_2} = \{(x, y, z) \in \partial\Omega | x \in \Omega \wedge y \in [0\text{m}, 1\text{m}] \wedge z = 2\text{m}\},$$

$$\Gamma_{D_3} = \{(x, y, z) \in \partial\Omega | x = 2\text{m} \wedge y \in \Omega \wedge z = [0\text{m}, 1\text{m}]\},$$

$$\Gamma_{D_4} = \{(x, y, z) \in \partial\Omega | x \in \Omega \wedge y = 2\text{m} \wedge z = [0\text{m}, 1\text{m}]\}.$$

The Dirichlet boundary condition on  $\Gamma_D$  results in the drainage process, whereas the Neumann boundary condition is applied on  $\Gamma_N = \partial\Omega \setminus \Gamma_D$ . The z-direction is point

downward into the ground. The initial conditions describing hydrostatic equilibrium are modified as follows:

$$\varphi(x, y, z, t) = \begin{cases} -2 + 2.2 \frac{t}{\Delta t_D} & \text{on } \Gamma_{D_1} \text{ and } \Gamma_{D_2}, T \leq \Delta t_D, \\ 0.2 & \text{on } \Gamma_{D_1} \text{ and } \Gamma_{D_2}, T > \Delta t_D, \\ 1 - z & \text{on } \Gamma_{D_3} \text{ and } \Gamma_{D_4}, \end{cases}$$

$$q(x, y, z, t) = 0 \text{ on } \Gamma_N,$$

$$\varphi(x, y, z, 0) = \begin{cases} 1 - z & \text{on } \Omega \setminus \Gamma_D, \\ -2 & \text{on } \Gamma_D. \end{cases}$$

We use the parameters listed in List (2016) to represent water flow dynamics in silt loam soil, in which  $\theta_s = 0.396$ ,  $\theta_r = 0.131$ ,  $\alpha = 0.423$ ,  $n = 2.06$ , and  $K_s = 0.0496$  in Equation (2). We choose  $\Delta t_D = \frac{1}{16}d$ ,  $\Delta t = \frac{1}{48}d$ , and  $T = \frac{3}{16}d$ . A rectangular 3-D mesh with 9261 nodes is used, where  $\Delta x = \Delta y = \Delta z = 0.1$ . The convergence tolerance  $\epsilon_0$  is set to be  $10^{-5}$ . Each MNN contains 3 layers and 10 neurons. Overall, 9261 noise-added reference solutions from global random walk solvers developed by Suciú et al. (2021) were obtained, with 70%, 15%, and 15% of them being used for training, validation, and testing, respectively. Bayesian regularization is used to train both MNNs.

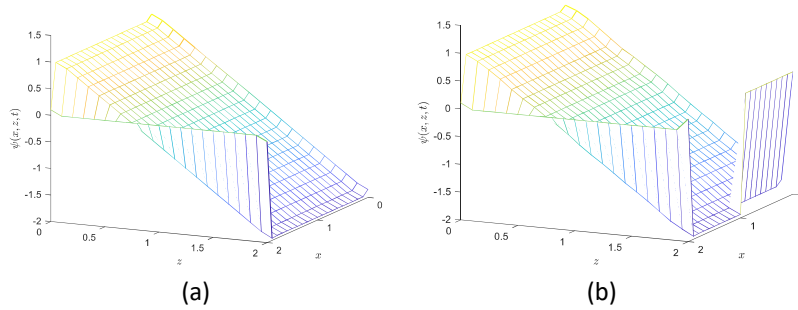


Figure 1. Pressure head obtained from (a) GRW algorithm, and (b) DGRW approach.

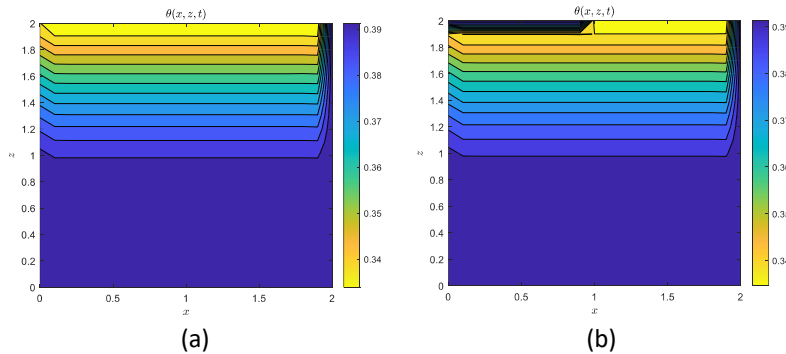


Figure 2. Pressure head obtained from (a) DGRW algorithm, and (b) GRW approach.

Figures 1 and 2 illustrate the pressure head and soil moisture results obtained using the GRW algorithm of Suciú et al. (2021) and our DGRW framework at  $y = 1.7m$  and  $t = T = \frac{3}{16}d$ . In general, our DGRW results show excellent agreement with the GRW results. Nevertheless, we observe that the GRW solutions did not produce jumps in pressure head and soil moisture content in the  $z$ -direction as  $x$  approaches  $1m$  ( $\Gamma_{D_1}$ ), whereas our

DGRW did predict these jumps. As the total simulated time is greater than  $\Delta t_D$ , the initial condition for pressure head should be 0.2m for  $x = [0\text{m}, 1\text{m}]$  and -2m for  $x = [1\text{m}, 2\text{m}]$  (Figure 1b). Similarly, jumps in soil moisture and flux in the  $z$ -direction are expected at  $x = 1\text{m}$  as well. Therefore, by effectively characterizing the complex relationship between pressure head and the number of particles, our DGRW approach is capable of capturing the water flow dynamics embedded in the Richards equation.

## 5. Conclusion

In this work, we propose a novel data-driven DGRW framework to accurately solve 3-D Richards equation for the first time. DGRW synergistically integrates data-driven global random walk theory and FVM to encapsulate physical knowledge and insights describing water flow dynamics in soil systems. We compare the solutions of our DGRW framework and state-of-the-art GRW approach on a 3-D benchmark problem and successfully validate the accuracy and usefulness of our approach in capturing the underlying physics of water flow dynamics.

## References

- Drought.gov, 2022, Current U.S. Drought Monitor Conditions for Oklahoma, <https://www.drought.gov/states/oklahoma>, accessed March 2022.
- R. Haverkamp, M. Vauclin, J. Touma, P.J. Wierenga, G. Vachaud, 1977, A comparison of numerical simulation models for one-dimensional infiltration, *Soil Science Society of America*, 41, 2, 285-294.
- K. Hornik, 1991, Approximation capabilities of multilayer feedforward networks, *Neural networks*, 4, 2, 251-257.
- K. Khand, S. Taghvaeian, A. Ajaz, 2018, Drought and Its Impact on Agricultural Water Resources in Oklahoma, <https://extension.okstate.edu/fact-sheets/drought-and-its-impact-on-agricultural-water-resources-in-oklahoma.html>, accessed March 2022.
- W. Lai, F.L. Ogden, 2015, A mass-conservative finite volume predictor–corrector solution of the 1D Richards’ equation, *Journal of Hydrology*, 523, 119-127.
- F.A. Radu, J.M. Nordbotten, I.S. Pop, K. Kumar, 2015, A robust linearization scheme for finite volume based discretizations for simulation of two-phase flow in porous media, *Journal of Computational and Applied Mathematics*, 289, 134-141.
- K. Rathfelder, L. M. Abriola, 1994, Mass conservative numerical solutions of the head-based richards equation, *Water Resources Research*, 30, 9, 2579-2586.
- L.A. Richards, 1931, Capillary conduction of liquids through porous mediums, *Physics*, 1, 5, 318-333.
- E. Sadler, R. Evans, K. Stone, and C. Camp, 2005, Opportunities for conservation with precision irrigation, *Journal of Soil and Water Conservation*, 60, 6, 371-378.
- Z. Song, Z. Jiang, 2023, A data-driven random walk approach for solving water flow dynamics in soil systems, In: *Proceedings Foundations of Computer-Aided Process Operations and Chemical Process Control Conference*. San Antonio, TX.
- N. Suci, D. Illiano, A. Prechtel, F.A. Radu, 2021, Global random walk solvers for fully coupled flow and transport in saturated/unsaturated porous media, *Advances in Water Resources*, 152, 103935.
- C. Vamos, N. Suci, H. Vereecken, O. Nitzsche, H. Hardelauf, 2001, Global random walk simulations of diffusion, In *Scientific Computing, Validated Numerics, Interval Methods*, pp. 343-354.
- M.T. van Genuchten, 1980, A closed-form equation for predicting the hydraulic conductivity of unsaturated soils, *Soil Science Society of America Journal*, 44, 5, 892-898.